Discussion Paper No.312

Time Delays and Chaos in Two Competing Species Revisited

Akio Matsumoto
Chuo University

Ferenc Szidarovszky
Corvinus University

April 2019

INSTITUTE OF ECONOMIC RESEARCH
Chuo University
Tokyo, Japan

Time Delays and Chaos in Two Competing Species Revisited*

Akio Matsumoto† Ferenc Szidarovszky‡

Abstract

This paper reexamines the Lotka-Volterra competition modelwith two delays. The steady state is shown to be locally asymptotically stable without delay. If the two delays are identical, then the model becomes a one-delay system. The critical value of the delay is determined when stability might be lost. If the delays are different, then the stability switching curves are analytically defined and numerically verified. It is demonstrated that the unstable two-delay system may exhibit periodic behavior, multistability, quasi period-doubling cascade and even complicated dynamics depending on model parameters.

Keywords: Lotka-Volterra system, Competition system, Two delays, Hopf bifurcation, Stabilliy loss and gain, Stability switching curve

*The first author highly acknowledges the financial supports from the Japan Society for the Promotion of Science (Grant-in-Aid for Scientific Research (C) 16K03556) and Chuo University (Grant for Special Research). The usual disclaimers apply.

†Professor, Department of Economics, Chuo University, 742-1, Higashi-Nakano, Hachioji, Tokyo, 192-0393, Japan; akiom@tamacc.chuo-u.ac.jp

‡Professor, Department of Mathematics, Corvinus University, Budapest, Fövám tér 8, 1093, Hungary; szidarka@gmail.com

1 Introduction

Shibata and Saito (1980, SS henceforth) consider a Lotka-Volterra competition system with two discrete time delays and numerically illustrate that this system can generate rich dynamic behavior including chaos. This paper revisits their study and reconsiders its dynamic structure from an analytical as well as a numerical point of view. In particular, it detects the roles of the two discrete time delays for the birth of various dynamics.

Their version is expressed as

$$\begin{aligned} \dot{x}(t) &= x(t)\left[\varepsilon_1 - a_{11}x(t-\tau_x) - a_{12}y(t)\right] \\ \dot{y}(t) &= y(t)\left[\varepsilon_2 - a_{21}x(t) - a_{22}y(t-\tau_y)\right] \end{aligned} \tag{1}$$

where $x(t)$ and $y(t)$ are the population densities of two competitive species at time t, ε_1 and ε_2 denote the intrinsic growth rates, τ_x and τ_y are maturation delays, the coefficients a_{ij} $(i,j=1,2)$ are all positive in the competition system. a_{ii} $(i=1,2)$ is the crowding coefficient measuring the strength of the intra-competition within species i whereas a_{ij} are the competition coefficients measuring the strength of the inter-competition between the species, i and j.[1] If there are no delays (i.e., $\tau_x = \tau_y = 0$), then system (1) is reduced to the Lotka-Volterra competition system where the stationary states are

$$\begin{aligned} x^e &= \frac{\varepsilon_1 a_{22} - \varepsilon_2 a_{12}}{a_{11}a_{22} - a_{12}a_{21}}, \\ y^e &= \frac{\varepsilon_2 a_{11} - \varepsilon_1 a_{21}}{a_{11}a_{22} - a_{12}a_{21}}. \end{aligned} \tag{2}$$

It is well-known that two species can coexist (i.e., $x^e > 0$ and $y^e > 0$) when the intra-competition dominates the inter-competition, that is,

$$\frac{a_{11}}{a_{21}} > \frac{\varepsilon_1}{\varepsilon_2} > \frac{a_{12}}{a_{22}}. \tag{3}$$

A delay system in biology has a long history. If there are no competitors (i.e., $a_{12} = a_{21} = 0$), then the population of each species is governed by the delay logistic equation that is called the Hutchinson equation (Hutchinson, 1948). May (1973) retains $\tau_x > 0$ but assumes away the delay of the species y, that is, $\tau_y = 0$ and discusses the delay effect on dynamics in the predator-prey system in which $\varepsilon_2 < 0$ and $\alpha_{21} < 0$. Shibata and Saito (1980) numerically show that the delay system (1) displays various dynamic behavior involving periodic solution and nonperiodic or chaotic solutions. In this study, we aim to provide an analytical underpinning for their numerical simulations. Further, we also numerically verify the analytical results using a *stability switching curve*.

Numerous attempts have been conducted on stability of variants of the delay Lotka-Volterra competition system. Song et al. (2004) replace the maturation

[1] Matsumoto and Szidarovszky (2019) consider a more general competition system in which the hunting delays are included such as $a_{12}y(t-\tau_y)$ and $a_{21}x(t-\tau_x)$.

delays with the hunting delays and show that the hunting delays are harmless. Zhang et al. (2009) study the occurrence of Hopf bifurcation when the maturation and hunting delays coexist and they are equal. Zhang (2012) is concerned with a slightly different version and discusses the stability of limit cycles emerged via the Hopf bifurcation. In this study, in addition to periodic behavior, we demonstrate that system (1) may give rise to the birth of complicated dynamics via quasi period-doubling cascade.[2]

The rest of the study is organized as follows. Section 2 establishes the stability condition of the non-delay Lotka-Volterra system as a benchmark. Section 3 examines a one-delay Lotka-Volterra model with $\tau_x = \tau_y = \tau$. Section 4, the main part of this study, derives a stability switching curve on which the competition system just loses stability under $\tau_x \neq \tau_y$. Section 5 performs some numerical simulations to reproduce Shibata-Saito's results and to ensure the analytical results. Section 6 concludes this study.

2 No-Delay Model

The steady state (2) with condition (3) is also the unique steady state of (1). To proceed to its stability, we linearize system (1) to obtain the homogeneous correspondence,

$$\begin{aligned} \dot{x}(t) &= -\alpha_x x(t-\tau_x) - \beta_x y(t) \\ \dot{y}(t) &= -\beta_y x(t) - \alpha_y y(t-\tau_y). \end{aligned} \tag{4}$$

where the new parameters are defined as

$$\alpha_x = a_{11}x^e,\ \alpha_y = a_{22}y^e,\ \beta_x = a_{12}x^e \text{ and } \beta_y = a_{21}y^e.$$

Assuming exponential solutions, $x(t) = e^{\lambda t}u$ and $y(t) = e^{\lambda t}v$ with constants $u \neq 0$ and $v \neq 0$, we obtain the corresponding characteristic equation,

$$P_0(\lambda) + P_1(\lambda)e^{-\lambda\tau_x} + P_2(\lambda)e^{-\lambda\tau_y} + P_3(\lambda)e^{-\lambda(\tau_x+\tau_y)} = 0 \tag{5}$$

where

$$P_0(\lambda) = \lambda^2 - \beta_x\beta_y,\ P_1(\lambda) = \alpha_x\lambda,\ P_2 = \alpha_y\lambda,\ P_3(\lambda) = \alpha_x\alpha_y.$$

For $\tau_x = \tau_y = 0$, the characteristic equation is reduced to

$$\lambda^2 + (\alpha_x + \alpha_y)\lambda + \left(\alpha_x\alpha_y - \beta_x\beta_y\right) = 0$$

where, due to (3),

$$\alpha_x\alpha_y - \beta_x\beta_y = (a_{11}a_{22} - a_{12}a_{21})\, x^e y^e > 0.$$

Positive coefficients imply that the stationary state with no delays is locally asymptotically stable. This result is well-known and summarized as follows.

[2] System (1) is considered to be a special version of Matsumoto and Szidarovszky (2019) However this study shows that system (1) can exhibit qualitatively different dynamics.

Theorem 1 *Given (3), the steady state of system (1) with* $\tau_x = \tau_y = 0$ *is locally asymptotically stable.*

3 One-Delay Model

We draw attention to the delay system but start with a simpler case in which system (1) has identical delays, $\tau_x = \tau_y = \tau > 0$. The corresponding characteristic equation is obtained from (5),

$$\lambda^2 - \beta_x\beta_y + (\alpha_x + \alpha_y)\,\lambda e^{-\lambda\tau} + \alpha_x\alpha_y e^{-2\lambda\tau} = 0$$

or multiplying both sides by $e^{-\lambda\tau}$ reduces it to

$$\left(\lambda^2 - \beta_x\beta_y\right) e^{\lambda\tau} + (\alpha_x + \alpha_y)\,\lambda + \alpha_x\alpha_y e^{-\lambda\tau} = 0. \tag{6}$$

It is apparent that $\lambda = 0$ is not a solution under condition (3). Inserting a possible solution $\lambda = i\omega$ with $\omega > 0$ for some τ into (6) and then separating the real and imaginary parts give

$$\begin{aligned} \left(\alpha_x\alpha_y - \beta_x\beta_y - \omega^2\right)\cos\omega\tau = 0, \\ \left(\alpha_x\alpha_y + \beta_x\beta_y + \omega^2\right)\sin\omega\tau - (\alpha_x + \alpha_y)\,\omega = 0. \end{aligned} \tag{7}$$

Define ω_* by $\omega_*^2 = \alpha_x\alpha_y - \beta_x\beta_y$ with which the first equation of (7) holds. The second equation with ω_* can be rewritten as

$$\sin\omega_*\tau = \frac{(\alpha_x + \alpha_y)\,\omega_*}{2\alpha_x\alpha_y}. \tag{8}$$

The condition for $|\sin\omega_*\tau| \le 1$ is

$$\omega_*^2 \le \frac{4\left(\alpha_x\alpha_y\right)^2}{\left(\alpha_x + \alpha_y\right)^2}$$

or using the definition of ω_*, it is transformed to

$$\alpha_x\alpha_y\left[1 - \frac{4\alpha_x\alpha_y}{\left(\alpha_x + \alpha_y\right)^2}\right] \le \beta_x\beta_y. \tag{9}$$

In Figure 1 in which $\beta_x\beta_y = 1$ is assumed,[3] the downward-sloping hyperbolic curve is described by $\alpha_x\alpha_y = \beta_x\beta_y$. The inequality condition (9) with $\alpha_x\alpha_y \ge \beta_x\beta_y$ is satisfied in the yellow region including the shaded one and violated in the green region whose boundary is described by the condition (9) with equality. Hence, the critical value of τ can be determined as

$$\tau_{*,m} = \frac{1}{\omega^*}\left[\sin^{-1}\left(\frac{(\alpha_x + \alpha_y)\,\omega_*}{2\alpha_x\alpha_y}\right) + 2m\pi\right] \text{ for } m = 0, 1, 2, \ldots\,. \tag{10}$$

[3] For any other values of $\beta_x\beta_y$, qualitatively the same figure can be obtained.

with

$$\omega_* = \sqrt{\alpha_x\alpha_y - \beta_x\beta_y} > 0.$$

Now suppose that $\omega^2 \neq \alpha_x\alpha_y - \beta_x\beta_y$. From the first equation of (7), we have

$$\cos\omega\tau = 0 \text{ and } \sin\omega\tau = \pm 1.$$

In case of $\sin\omega\tau = -1$, the second equation of (7) is

$$\omega^2 + (\alpha_x + \alpha_y)\,\omega + \left(\alpha_x\alpha_y + \beta_x\beta_y\right) = 0.$$

Since $\alpha_x + \alpha_y > 0$ and $\alpha_x\alpha_y + \beta_x\beta_y > 0$, the real parts of the solutions are negative. Hence no stability switch occurs and the delay is *harmless*. We eliminate this case for further consideration. On the other hand, in case of $\sin\omega\tau = +1$, the second equation is

$$\omega^2 - (\alpha_x + \alpha_y)\,\omega + \left(\alpha_x\alpha_y + \beta_x\beta_y\right) = 0. \tag{11}$$

The solutions are positive,

$$\omega_\pm = \frac{1}{2}\left[\alpha_x + \alpha_y \pm \sqrt{D}\right]$$

where the discriminant D is

$$D \quad = (\alpha_x - \alpha_y)^2 - \left(2\sqrt{\beta_x\beta_y}\right)^2.$$

The conditions for the non-negative D are

$$\alpha_y \leq \alpha_x - 2\sqrt{\beta_x\beta_y} \text{ or } \alpha_y \geq \alpha_x + 2\sqrt{\beta_x\beta_y}. \tag{12}$$

Solving $\cos\omega\tau = 0$ gives the critical values of the delay,

$$\tau_{+,n} = \frac{1}{\omega_+}\left(\frac{\pi}{2} + 2n\pi\right) \text{ and } \tau_{-,n} = \frac{1}{\omega_-}\left(\frac{\pi}{2} + 2n\pi\right) \text{ for } n = 0, 1, 2, \ldots\ .$$

and

$$0 < \tau_{+,0} < \tau_{-,0}.$$

In the yellow region bounded by the two lines, the discriminant is negative and thus we have the following result concerning stability switching:

Lemma 2 *In the yellow region in which $D < 0$, the steady state of system (1) with $\tau_x = \tau_y = \tau$ is locally asymptotically stable for $\tau < \tau_{*,0}$ and unstable for $\tau > \tau_{*,0}$ where*

$$\tau_{*,0} = \frac{1}{\omega^*}\sin^{-1}\left[\frac{(\alpha_x + \alpha_y)\,\omega^*}{2\alpha_x\alpha_y}\right].$$

On the other hand, in the green region we have the following:

Lemma 3 *In the green region in which condition (9) is violated, the steady state of system (1) with $\tau_x = \tau_y = \tau$ is locally asymptotically stable for $\tau < \tau_{+,0}$ and unstable for $\tau > \tau_{+,0}$ where*

$$\tau_{+,0} = \frac{\pi}{2\omega_+}$$

Let us denote the left hand side expressions of the second equation of (7) and (11) by $f(\omega)$ and $g(\omega)$, respectively,

$$f(\omega) = \sin\omega\tau \cdot \omega^2 - (\alpha_x + \alpha_y)\omega + \sin\omega\tau(\alpha_x\alpha_y + \beta_x\beta_y)$$

and

$$g(\omega) = \omega^2 - (\alpha_x + \alpha_y)\,\omega + \left(\alpha_x\alpha_y + \beta_x\beta_y\right).$$

Subtracting $f(\omega)$ from $g(\omega)$ yields

$$g(\omega) - f(\omega) = \left[\omega^2 + \left(\alpha_x\alpha_y + \beta_x\beta_y\right)\right](1 - \sin\omega\tau) > 0 \text{ unless } \sin\omega\tau = 1.$$

It has been verified that

$$f(\omega_*) = 0 \text{ and } g(\omega_\pm) = 0$$

and

$$\sin\omega_*\tau_{*,0} < 1 \text{ and } \sin\omega_+\tau_{+,0} = 1.$$

The inequality $g(\omega) > f(\omega)$ implies

$$\omega_+ < \omega_*$$

and consequently

$$\tau_{*,0} < \tau_{+,0}.$$

Hence we have the following result:

Lemma 4 *In the shaded yellow region in which condition (9) holds and $D > 0$, the critical value determining stability switching is $\tau_{*,0}$ implying that the steady state of system (1) with $\tau_x = \tau_y = \tau$ is locally asymptotically stable for $\tau < \tau_{*,0}$ and unstable for $\tau > \tau_{*,0}$*

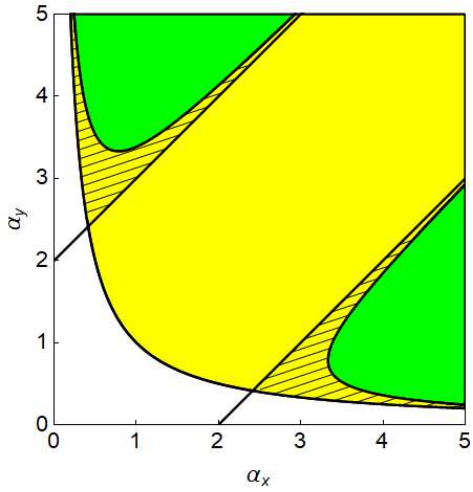

Figure 1. Stability regions for system (1) with $\tau_x = \tau_y = \tau$.

4 Two Delay Model

We now suppose $\tau_x > 0$, $\tau_y > 0$ and $\tau_x \neq \tau_y$ and consider how such delays affect stability of model (4). We can see that $\lambda = 0$ is not a solution of the characteristic equation (5) and thus look for purely complex roots. To this end, we assume that $\lambda = i\omega$ with $\omega > 0$ again. Then the characteristic equation is changed to

$$P_0(i\omega) + P_1(i\omega)e^{-i\omega\tau_x} + P_2(i\omega)e^{-i\omega\tau_y} + P_3(i\omega)e^{-i\omega(\tau_x+\tau_y)} = 0 \tag{13}$$

where

$$P_0(i\omega) = -\omega^2 - \beta_x\beta_y,\ P_1(i\omega) = i\alpha_x\omega,\ P_2(i\omega) = i\alpha_y\omega,\ P_3(i\omega) = \alpha_x\alpha_y. \tag{14}$$

Applying the method developed by Matsumoto and Szidarovszky (2018) that is based on Lin and Wang (2012), we derive the conditions of τ_x and τ_y under which the characteristic roots are purely complex. Equation (13) can be rewritten as

$$P_0(i\omega) + P_1(i\omega)e^{-i\omega\tau_x} + \left[P_2(i\omega) + P_3(i\omega)e^{-i\omega\tau_x}\right] e^{-i\omega\tau_y} = 0. \tag{15}$$

Science $\left|e^{-i\omega\tau_y}\right| = 1$, equation (15) has solution for τ_x if and only if

$$\left|P_0(i\omega) + P_1(i\omega)e^{-i\omega\tau_x}\right| = \left|P_2(i\omega) + P_3(i\omega)e^{-i\omega\tau_x}\right|$$

or squaring both sides generates the equivalent forms,

$$(P_0(i\omega) + P_1(i\omega)e^{-i\omega\tau_x})(\bar{P}_0(i\omega) + \bar{P}_1(i\omega)e^{i\omega\tau_x})$$

$$= (P_2(i\omega) + P_3(i\omega)e^{-i\omega\tau_x})(\bar{P}_2(i\omega) + \bar{P}_3(i\omega)e^{i\omega\tau_x})$$

where over-bar indicates complex conjugate. After some calculations, this equation can be reduced to

$$|P_0|^2 + |P_1|^2 - |P_2|^2 - |P_3|^2 = 2A_x(\omega)\cos\omega\tau_x - 2B_x(\omega)\sin\omega\tau_x \tag{16}$$

where the argument of P_i is omitted for notational simplicity. In the right hand side of this equation, we have

$$A_x(\omega) = \mathrm{Re}\left[P_2\bar{P}_3 - P_0\bar{P}_1\right] = 0$$

and

$$B_x(\omega) = \mathrm{Im}\left[P_2\bar{P}_3 - P_0\bar{P}_1\right] = \alpha_x\omega\left(\alpha_y^2 - \beta_x\beta_y - \omega^2\right) \tag{17}$$

where $P_k(\omega)$ for $k = 0, 1, 2, 3$ in (14) are used. Then equation (16) is reduced to

$$|P_0|^2 + |P_1|^2 - |P_2|^2 - |P_3|^2 = -2B_x(\omega)\sin\omega\tau_x. \tag{18}$$

Returning to equation (13), we can transform it in a different way,

$$P_0 + P_2e^{-i\omega\tau_y} + \left[P_1 + P_3e^{-i\omega\tau_y}\right]e^{-i\omega\tau_x} = 0. \tag{19}$$

Then using exactly the same idea as before, we can arrive at the following form:

$$|P_0|^2 - |P_1|^2 + |P_2|^2 - |P_3|^2 = -2B_y(\omega)\sin\omega\tau_y \tag{20}$$

where

$$B_y(\omega) = \alpha_y\omega\left(\alpha_x^2 - \beta_x\beta_y - \omega^2\right). \tag{21}$$

To find an appropriate pair of τ_x and τ_y satisfying equation (13), we examine first the case of $B_x(\omega) = 0$ and $B_y(\omega) = 0$ and then proceed to the case of $B_x(\omega) \neq 0$ or $B_y(\omega) \neq 0$.

4.1 Case 1: $B_x(\omega) = 0$ and $B_y(\omega) = 0$

Let ω_x and ω_y be positive solutions of $B_x(\omega) = 0$ and $B_y(\omega) = 0$,

$$\omega_x^2 = \alpha_y^2 - \beta_x\beta_y$$

and

$$\omega_y^2 = \alpha_x^2 - \beta_x\beta_y.$$

We denote the left hand sides of (18) and (20) by $f_x(\omega)$ and $f_y(\omega)$ and then rewrite them by using (14),

$$f_x(\omega) = \omega^4 + \left(2\beta_x\beta_y + \alpha_x^2 - \alpha_y^2\right)\omega^2 - \left[(\alpha_x\alpha_y)^2 - \left(\beta_x\beta_y\right)^2\right]$$

$$f_y(\omega) = \omega^4 + \left(2\beta_x\beta_y - \alpha_x^2 + \alpha_y^2\right)\omega^2 - \left[(\alpha_x\alpha_y)^2 - \left(\beta_x\beta_y\right)^2\right].$$

Solving $f_x(\omega) = 0$ and $f_y(\omega) = 0$ for ω^2 gives

$$\omega_{x\pm}^2 = \frac{\alpha_y^2 - \alpha_x^2 - 2\beta_x\beta_y \pm \sqrt{\left(\alpha_x^2 + \alpha_y^2\right)^2 + 4\beta_x\beta_y\left(\alpha_x^2 - \alpha_y^2\right)}}{2}$$

and

$$\omega_{y\pm}^2 = \frac{\alpha_x^2 - \alpha_y^2 - 2\beta_x\beta_y \pm \sqrt{\left(\alpha_x^2 + \alpha_y^2\right)^2 + 4\beta_x\beta_y\left(\alpha_y^2 - \alpha_x^2\right)}}{2}.$$

Apparently both solutions are identical, $\omega_x^2 = \omega_{x+}^2$ and $\omega_y^2 = \omega_{y+}^2$, if $\alpha_x = \alpha_y$ whereas they are different, $\omega_x^2 \neq \omega_{x+}^2$ and $\omega_y^2 \neq \omega_{y+}^2$, if $\alpha_x \neq \alpha_y$. We impose the slightly stronger conditions only for notational simplicity and then find the pair of (τ_x, τ_y) for the characteristic equation (13).

Assumption 2. $\alpha_x = \alpha_y = \alpha$ and $\beta_x = \beta_y = \beta$.

Assumptions 2 leads to

$$B_x(\omega) = B_y(\omega) = \alpha\omega(\alpha^2 - \beta^2 - \omega^2).$$

Consequently the solution for $B_x(\omega) = 0$ and $B_y(\omega) = 0$ is

$$\omega^* = \sqrt{\alpha^2 - \beta^2} > 0$$

where the inequality is due to Assumption 1. Also under Assumption 2, the two species are symmetric so that we focus on the first one henceforth. Equation (15) can be reduced to

$$e^{-i\omega\tau_y} = -\frac{P_0(i\omega) + P_1(i\omega)e^{-i\omega\tau_x}}{P_2(i\omega) + P_3(i\omega)e^{-i\omega\tau_x}}. \tag{22}$$

We use the Euler's formula for the left hand side and rationalize the denominator of the right hand side to have

$$\cos\omega\tau_y - i\sin\omega\tau_y = -\frac{m_x}{d_x} - i\frac{n_x}{d_x} \tag{23}$$

where

$$d_x = \alpha^2\left[\left(\cos\omega\tau_x\right)^2 + \left(\omega - \alpha\sin\omega\tau_x\right)^2\right] > 0$$

$$m_x = -\left(\alpha\beta\right)^2\cos\omega\tau_x \tag{24}$$

and

$$n_x = \alpha\left[2\alpha^2\omega - \alpha\left(2\alpha^2 - \beta^2\right)\sin\omega\tau_x\right] \tag{25}$$

Comparing both sides, we have

$$\cos\omega\tau_y = -\frac{m_x}{d_x} \text{ and } \sin\omega\tau_y = \frac{n_x}{d_x}. \tag{26}$$

For further development, we need to specify the parameter values. So we take the same specification that is adopted by Shibata and Saito (1980).

Specification I. $a_{11} = a_{22} = 2,\ a_{12} = a_{21} = 1$ and $\varepsilon_1 = \varepsilon_2 = 2$.

With Specification 1, the reduced parameters have the following values,

$$\alpha_x = \alpha_y = \alpha = \frac{4}{3} \text{ and } \beta_x = \beta_y = \beta = \frac{2}{3}.$$

The graphs of $-m_x/d_x$ and n_x/d_x are illustrated as red and blue curves for $\tau_x \in (0, 2\pi/\omega^*)$ in Figure 1. The red curve intersects the horizontal axis twice at which $m_x = 0$ or $\cos\omega^*\tau_x = 0$ from (24). Hence we have $\omega^*\tau_x = \pi/2$ at point B and $\omega^*\tau_x = 3\pi/2$ at point D,

$$\tau_x^B = \frac{\pi}{2\omega^*} \simeq 1.36 \text{ and } \tau_x^D = \frac{3\pi}{2\omega^*} \simeq 4.08.$$

It is also seen that the blue curve intersects the horizontal axis twice at which $n_x = 0$ or from (25)

$$\sin\omega^*\tau_x = \frac{2\alpha\omega}{2\alpha^2 - \beta^2} = \frac{8\sqrt{3}}{14} \simeq 0.9897 < 1.$$

Since points A and C are left, respectively, right to point B and $\sin\omega^*\tau_x$ takes the maximum value $+1$ at point B with $\omega^*\tau_x^B = \pi/2$, we have $\omega^*\tau_x^A < \pi/2$ at point A at which $\cos\omega^*\tau_x^A > 0$ and $\omega^*\tau_x^C > \pi/2$ at point C at which $\cos\omega^*\tau_x^C < 0$. Hence

$$\tau_x^A = \frac{1}{\omega^*}\sin^{-1}\left(\frac{8\sqrt{3}}{14}\right) \simeq 1.24$$

and

$$\tau_x^C = \frac{1}{\omega^*}\left[\pi - \sin^{-1}\left(\frac{8\sqrt{3}}{14}\right)\right] \simeq 1.48.$$

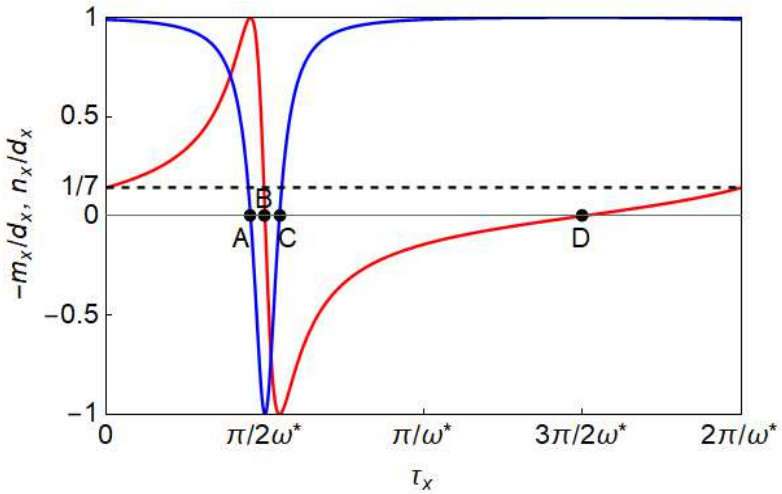

Figure 2. Graphs of $-m_x/d_x$ (red) and n_x/d_x (blue)

The interval $[0, 2\pi/\omega^*]$ is divided into five subintervals. In the first subinterval $(0, \tau_x^A)$, it is seen that $\cos\omega^*\tau_y > 0$ and $\sin\omega^*\tau_y > 0$. Hence, from (26), solving $\cos\omega^*\tau_y = -m_x/d_x$ and $\sin\omega^*\tau_y = n_x/d_x$ for τ_y determines the corresponding values of τ_y satisfying equation (22),

$$\tau_y^c(\tau_x) = \frac{1}{\omega^*}\cos^{-1}\left(-\frac{m_x}{d_x}\right) \text{ and } \tau_y^s(\tau_x) = \frac{1}{\omega^*}\sin^{-1}\left(\frac{n_x}{d_x}\right) \tag{27}$$

where the superscripts c and s stand for cos and sin, respectively. In the same way, we have $\cos\omega^*\tau_y > 0$ and $\sin\omega^*\tau_y < 0$ for $\tau_x \in \left(\tau_x^A, \tau_x^B\right)$ in which

$$\tau_y^c(\tau_x) = \frac{1}{\omega^*}\left[\pi + \cos^{-1}\left(\frac{m_x}{d_x}\right)\right] \text{ and } \tau_y^s(\tau_x) = \frac{1}{\omega^*}\left[2\pi + \sin^{-1}\left(\frac{n_x}{d_x}\right)\right]. \tag{28}$$

For $\tau_x \in \left(\tau_x^B, \tau_x^C\right)$, $\cos\omega^*\tau_y < 0$ and $\sin\omega^*\tau_y < 0$ imply

$$\tau_y^c(\tau_x) = \frac{1}{\omega^*}\left[\pi + \cos^{-1}\left(\frac{m_x}{d_x}\right)\right] \text{ and } \tau_y^s(\tau_x) = \frac{1}{\omega^*}\left[\pi - \sin^{-1}\left(\frac{n_x}{d_x}\right)\right]. \tag{29}$$

For $\tau_x \in \left(\tau_x^C, \tau_x^D\right)$, $\cos\omega^*\tau_y < 0$ and $\sin\omega^*\tau_y > 0$ imply

$$\tau_y^c(\tau_x) = \frac{1}{\omega^*}\cos^{-1}\left(-\frac{m_x}{d_x}\right) \text{ and } \tau_y^s(\tau_x) = \frac{1}{\omega^*}\left[\pi - \sin^{-1}\left(\frac{n_x}{d_x}\right)\right]. \tag{30}$$

Finally, we have $\cos\omega^*\tau_y > 0$ and $\sin\omega^*\tau_y > 0$ for $\tau_x \in \left(\tau_x^D, 2\pi/\omega^*\right)$ as in the first subinterval,

$$\tau_y^c(\tau_x) = \frac{1}{\omega^*}\cos^{-1}\left(-\frac{m_x}{d_x}\right) \text{ and } \tau_y^s(\tau_x) = \frac{1}{\omega^*}\left[\sin^{-1}\left(\frac{n_x}{d_x}\right)\right]. \tag{31}$$

Since $\tau_y^c(\tau_x) = \tau_y^s(\tau_x)$ holds for $\tau_x \in [0, 2\pi/\omega^*]$, the solution can be denoted by $\tau_y(\tau_x)$.

The locus of $(\tau_x, \tau_y(\tau_x))$ for $\tau_x \in [0, 2\pi/\omega^*]$ constructs the crossing curves in case of $B_x(\omega) = 0$ that are illustrated by two black-red curves in Figure 3. More precisely, the inner concave-shaped black segment is described by (27) whereas the outer convex-shaped curve consists of four segments, from left to right, the upper-most red segment by (28), the black segment by (29), the red segment with strong curvature by (30) and the right-most black segment by (31). The results obtained so far are summarized as follows:

Theorem 5 *If $B_x(\omega) = 0$ for $\omega = \omega^*$, $\alpha_x = \alpha_y = \alpha$, $\beta_x = \beta_y = \beta$ and $\alpha > \beta$, then the crossing curve is described by the locus of $(\tau_x, \tau_y(\tau_x))$ where*

$$\tau_y(\tau_x) = \frac{1}{\omega^*}\cos^{-1}\left(-\frac{m_x}{d_x}\right) \text{ for } \tau_x \in (0, \tau_x^A) \cup \left(\tau_x^C, \tau_x^D\right) \cup \left(\tau_x^D, 2\pi/\omega^*\right)$$

and

$$\tau_y(\tau_x) = \frac{1}{\omega^*}\left[\pi + \cos^{-1}\left(\frac{m_x}{d_x}\right)\right] \text{ for } \tau_x \in \left(\tau_x^A, \tau_x^B\right) \cup \left(\tau_x^B, \tau_x^C\right)$$

where

$$\omega^* = \sqrt{\alpha^2 - \beta^2} > 0.$$

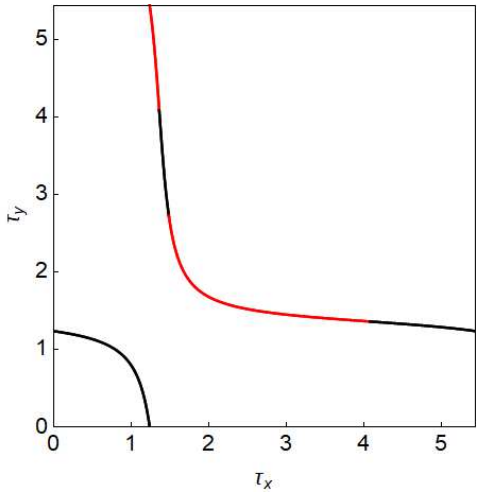

Figure 3. Crossing curves in case of $\alpha_x = \alpha_y = \alpha$ and $\beta_x = \beta_y = \beta$

4.2 Case 2: $|B_x(\omega)| > 0$ and $|B_y(\omega)| > 0$

In this section we assume away Assumption 2 and consider the case in which $B_x(\omega) \neq 0$ and $B_y(\omega) \neq 0$. We first focus on $B_x(\omega)$ that can be written as

$$B_x(\omega) = \alpha_x \omega \left(\omega_x + \omega\right)\left(\omega_x - \omega\right)$$

with

$$\omega_x = \sqrt{\alpha_y^2 - \beta_x \beta_y}.$$

It can be checked that there exist $\varphi_x(\omega)$ such that

$$\varphi_x(\omega) = \arg\left[P_2\bar{P}_3 - P_0\bar{P}_1\right] = \begin{cases} \dfrac{\pi}{2} & \text{if } B_x(\omega) > 0 \text{ or } \omega < \omega_x \\ \dfrac{3\pi}{2} & \text{if } B_x(\omega) < 0 \text{ or } \omega > \omega_x \end{cases}$$

implying that

$$\sin\left[\varphi_x(\omega)\right] = \frac{B_x(\omega)}{\sqrt{B_x(\omega)^2}} = 1 \text{ and } \cos\left[\varphi_x(\omega)\right] = \frac{A_x(\omega)}{\sqrt{B_x(\omega)^2}} = 0$$

Rewriting the first equation as

$$B_x(\omega) = \sqrt{B_x(\omega)^2}\sin\left[\varphi_x(\omega)\right]$$

and using the addition theorem, we obtain

$$|P_0|^2 + |P_1|^2 - |P_2|^2 - |P_3|^2 = 2\sqrt{B_x(\omega)^2}\cos\left[\varphi_x(\omega) + \omega\tau_x\right]. \tag{32}$$

Then we have

$$\frac{|P_0|^2 + |P_1|^2 - |P_2|^2 - |P_3|^2}{2\sqrt{B_x(\omega)^2}} = \cos\left[\varphi_x(\omega) + \omega\tau_x\right] \leq 1. \tag{33}$$

Hence a sufficient and necessary condition for the existence of $\tau_x > 0$ satisfying the above equation is

$$\left||P_0|^2 + |P_1|^2 - |P_2|^2 - |P_3|^2\right| \leq 2\sqrt{B_x(\omega)^2}$$

or

$$F(\omega) = \left(|P_0|^2 + |P_1|^2 - |P_2|^2 - |P_3|^2\right)^2 - 4\left[B_x(\omega)\right]^2 \leq 0.$$

With $P_k(i\omega)$ for $k = 0, 1, 2, 3$ and a new variable $x = \omega^2$, $F(\omega)$ can be transformed to

$$F(x) = x^4 + a_3x^3 + a_2x^2 + a_1x + x_0 \tag{34}$$

where

$$a_3 = -2\left(\alpha_x^2 + \alpha_y^2 - 2\beta_x\beta_y\right),$$

$$a_2 = \alpha_x^4 + \alpha_y^4 + 4\left(\alpha_x\alpha_y\right)^4 - 2\beta_x\beta_y\left(2\alpha_x^2 + 2\alpha_y^2 - 3\beta_x\beta_y\right),$$

$$a_1 = -2\left(\alpha_x^2 + \alpha_y^2 - 2\beta_x\beta_y\right),$$

$$a_0 = \left(\alpha_x\alpha_y - \beta_x\beta_y\right)^2\left(\alpha_x\alpha_y + \beta_x\beta_y\right)^2.$$

This fourth order polynomial can be factorized as

$$x^4 + a_3x^3 + a_2x^2 + a_1x + x_0 = F_1(x)F_2(x)$$

where

$$F_1(x) = x^2 - \left(\alpha_x^2 + \alpha_y^2 - 2\beta_x\beta_y\right)x + \left(\alpha_x\alpha_y - \beta_x\beta_y\right)^2$$

and

$$F_2(x) = x^2 - \left(\alpha_x^2 + \alpha_y^2 - 2\beta_x\beta_y\right)x + \left(\alpha_x\alpha_y + \beta_x\beta_y\right)^2.$$

Solving $F_1(x) = 0$ yields two solutions,

$$x_1 = \frac{1}{2}\left\{\alpha_x^2 + \alpha_y^2 - 2\beta_x\beta_y - (\alpha_x - \alpha_y)\sqrt{(\alpha_x + \alpha_y)^2 - 4\beta_x\beta_y}\right\} \tag{35}$$

and

$$x_2 = \frac{1}{2}\left\{\alpha_x^2 + \alpha_y^2 - 2\beta_x\beta_y + (\alpha_x - \alpha_y)\sqrt{(\alpha_x + \alpha_y)^2 - 4\beta_x\beta_y}\right\} \tag{36}$$

where the discriminant is positive,

$$(\alpha_x + \alpha_y)^2 - 4\beta_x\beta_y = (\alpha_x - \alpha_y)^2 + 4\left(\alpha_x\alpha_y - \beta_x\beta_y\right) > 0.$$

Solving $F_2(x) = 0$ also yields two solutions,

$$x_3 = \frac{1}{2}\left\{\alpha_x^2 + \alpha_y^2 - 2\beta_x\beta_y - (\alpha_x + \alpha_y)\sqrt{D}\right\} \tag{37}$$

and

$$x_4 = \frac{1}{2}\left\{\alpha_x^2 + \alpha_y^2 - 2\beta_x\beta_y + (\alpha_x + \alpha_y)\sqrt{D}\right\}. \tag{38}$$

where

$$D = (\alpha_x - \alpha_y)^2 - 4\beta_x\beta_y \gtreqless 0. \tag{39}$$

The discriminant can have either sign, depending on the parameter specification,

$$D > 0 \text{ if } |\alpha_y - \alpha_x| > 2\sqrt{\beta_x\beta_y}$$

and

$$D < 0 \text{ if } |\alpha_y - \alpha_x| < 2\sqrt{\beta_x\beta_y}.$$

Lemma 6 *If $\alpha_x = \alpha_y$, then $F(\omega) \geq 0$ for any $\omega \geq 0$.*

Proof. (35) and (36) imply $x_1 = x_2$ if $\alpha_x = \alpha_y$ and $F_1(x) > 0$ otherwise. (39) implies $D < 0$ leading to $F_2(x) > 0$ for any $x \geq 0$. ■

This lemma implies that there is no ω making $F(\omega) < 0$. Therefore no stability switch occurs in case of $|B_x(\omega)| > 0$.

Subtracting $F_2(x)$ from $F_1(x)$ presents

$$F_1(x) - F_2(x) = -4\alpha_x\alpha_y\beta_x\beta_y < 0.$$

The inequality leads to the following two results where ω_i is the positive solution of $\omega_i^2 = x_i$ for $i = 1, 2, 3, 4$.

Lemma 7 *If $|\alpha_y - \alpha_x| < 2\sqrt{\beta_x\beta_y}$, then $F(\omega) < 0$ for $\omega \in (\omega_1, \omega_2)$.*

Proof. $F_2(x) > 0$ always and $F_1(x) < 0$ for $x \in (x_1, x_2)$ and $F_1(x) \geq 0$ otherwise. ■

Lemma 8 *If $|\alpha_y - \alpha_x| > 2\sqrt{\beta_x\beta_y}$, then $F(\omega) < 0$ for $\omega \in (\omega_1, \omega_3) \cup (\omega_4, \omega_1)$.*

Proof. It is clear that $F_1(x) < 0$ and $F_2(x) > 0$ for $x \in (x_1, x_3) \cup (x_4, x_1)$ and $F_1(x) \geq 0$ and $F_2(x) \geq 0$ otherwise. ■

Let us define $\psi_x(\omega)$ by

$$\psi_x(\omega) = \cos^{-1}\left[\frac{|P_0|^2 + |P_1|^2 - |P_2|^2 - |P_3|^2}{2\sqrt{B_x(\omega)^2}}\right].$$

Comparing this expression with (33) determines the critical values of delay τ_x,

$$\tau_{x,m}^{\pm} = \frac{1}{\omega}\left[\pm\psi_x(\omega) - \varphi_x(\omega) + 2m\pi\right] \text{ for } m = 0, 1, 2, ... \tag{40}$$

We now draw attention to the case of $B_y(\omega) \neq 0$ to determine the corresponding values of delay τ_y. We return to the characteristic equation (13) and alternatively put it as

$$P_0(i\omega) + P_2(i\omega)e^{-i\omega\tau_y} + \left[P_1(i\omega) + P_3(i\omega)e^{-i\omega\tau_y}\right]e^{-i\omega\tau_x} = 0. \tag{41}$$

The similarity of (41) to (15) is clear. Hence, in the same way as before, we can derive the critical value of τ_y as

$$\tau_{y,n}^{\pm} = \frac{1}{\omega}\left[\pm\psi_y(\omega) - \varphi_y(\omega) + 2n\pi\right] \text{ for } n = 0, 1, 2, ... \tag{42}$$

where

$$A_y(\omega) = \mathrm{Re}\left[P_1\bar{P}_3 - P_0\bar{P}_2\right] = 0,$$

$$B_y(\omega) = \mathrm{Im}\left[P_1\bar{P}_3 - P_0\bar{P}_2\right] = \alpha_y\omega\left[\alpha_x^2 - \beta_x\beta_y - \omega^2\right],$$

$$\psi_y(\omega) = \cos^{-1}\left[\frac{|P_0|^2 - |P_1|^2 + |P_2|^2 - |P_3|^2}{2\sqrt{B_y(\omega)^2}}\right]$$

and

$$\varphi_y(\omega) = \arg\left[P_1\bar{P}_3 - P_0\bar{P}_2\right] = \begin{cases} \dfrac{\pi}{2} & \text{if } B_y(\omega) > 0 \text{ or } \omega < \omega_y, \\ \dfrac{3\pi}{2} & \text{if } B_y(\omega) < 0 \text{ or } \omega > \omega_y \end{cases}$$

with ω_y being a positive solution of $B_y(\omega) = 0$. In case of $B_y(\omega) = 0$, we solve (41) to have

$$e^{-i\omega\tau_x} = -\frac{P_0(i\omega) + P_2(i\omega)e^{-i\omega\tau_y}}{P_1(i\omega) + P_3(i\omega)e^{-i\omega\tau_y}}. \tag{43}$$

We can derive $\tau_x(\tau_y)$ from (43) in the same way as deriving $\tau_y(\tau_x)$ from (22). Since equations (22) and (43) are different expression for the same characteristic

equation (13), the crossing curve $(\tau_x(\tau_y), \tau_y)$ is identical with the crossing curve $(\tau_x, \tau_y(\tau_x))$. Concerning $\varphi_y(\omega)$, we need a condition similar to $F(\omega)$,

$$G(\omega) = \left||P_0|^2 - |P_1|^2 + |P_2|^2 - |P_3|^2\right|^2 - 4B_y(\omega)^2 \leq 0.$$

Since $F(\omega) = G(\omega)$, the solutions of $F(\omega) = 0$ also solve $G(\omega) = 0$ although the positive solution of $B_x(\omega) = 0$ is different from the solution of $B_y(\omega) = 0$,

$$\omega_x \lessgtr \omega_y \text{ according to } \alpha_x \gtrless \alpha_y.$$

Under Specification 1, Theorem 5 indicates that the stability switching curve is described by equation (27), that is, the inner concave-shaped curve that is reproduced in Figure 4(A). This curve corresponds to the concave curve in Figure 1 of Shibata and Saito (1980, p.202) in which no derivations for their curve are given.

Specification II. $a_{11} = 2,\ a_{12} = 5/2,\ a_{12} = a_{21} = 1$ and $\varepsilon_1 = \varepsilon_2 = 2$.

Under Specification II, the reduced parameters take the following values,

$$\alpha_x = \frac{3}{2} > \alpha_y = \frac{5}{4},\ \beta_x = \frac{3}{4} \text{ and } \beta_y = \frac{1}{2}.$$

It is confirmed that $\alpha_y > \alpha_x - 2\sqrt{\beta_x\beta_y}$, implying that $F(\omega) = 0$ as well as $G(\omega) = 0$ has two solutions,

$$\omega_1 \simeq 1.106 \text{ and } \omega_2 \simeq 1.356,$$

Further, solving $B_x(\omega) = 0$ and $B_y(\omega) = 0$ yields solutions,

$$\omega_x \simeq 1.089 \text{ and } \omega_y \simeq 1.369.$$

Hence we have

$$\omega_x < \omega_1 < \omega_2 < \omega_y$$

implying that

$$B_x(\omega) = \frac{3\pi}{2} \text{ and } B_y(\omega) = \frac{\pi}{2} \text{ for } \omega \in (\omega_1, \omega_2)\,.$$

The stability switching curves are described by two segments,

$$\left(\tau^+_{x,0}(\omega), \tau^-_{y,1}(\omega)\right) \text{ and } \left(\tau^-_{x,1}(\omega), \tau^+_{y,0}(\omega)\right) \text{ for } \omega \in (\omega_1, \omega_2)$$

where $\tau^+_{x,0}(\omega)$ of the former segment takes negative values, so only the latter segment is illustrated in Figure 4(B). Notice that in Figures 4(A) and 4(B), we

use the same notation for the points on the vertical and horizontal axes only for notational simplicity.[4]

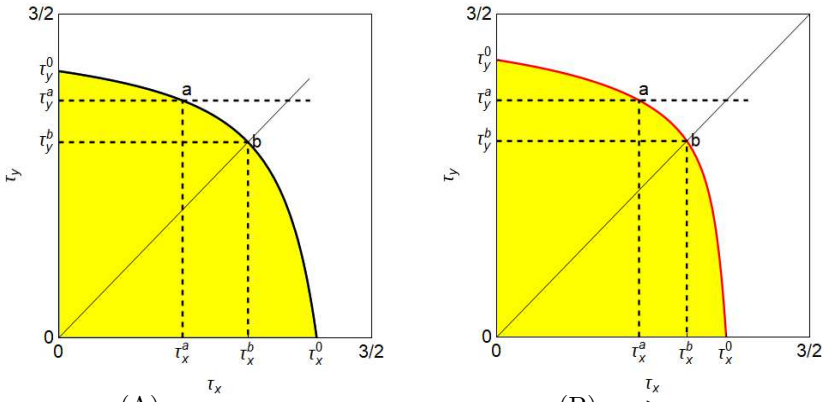

(A) $\alpha_x = \alpha_y$ (B) $\alpha_x > \alpha_y$

Figure 4. Stability regions

5 Numerical Simulations

This section is divided into two parts. Numerical simulations under $\alpha_x = \alpha_y$ are performed in the first part and those under $\alpha_x > \alpha_y$ in the second part.

5.1 Symmetric Case

Specification I is adopted in this subsection, with which the two species are symmetric. In the first example, we assume the identical delays, $\tau_x = \tau_y = \tau$ and simulate system (1) for $0 \leq t \leq T(= 2000)$ by increasing the value of the delay along the diagonal of Figure 4(A). Two simulations are performed with different initial functions.[5] The red bifurcation diagram in Figure 5 is obtained when the initial functions defined for $t \leq 0$ are different,

$$\phi_x(t) = x^e + 0.2 \text{ and } \phi_y(t) = y^e + 0.1$$

[4] In partitular, in Figure 4(A)

$$\tau_y^0 \simeq 1.236,\ \tau_y^a = 1.1, \tau_y^b \simeq 0.907$$

and

$$\tau_x^a \simeq 0.594,\ \tau_x^b \simeq 0.907, \tau_x^b \simeq 1.236.$$

On the other hand, in Figure 4(B)

$$\tau_y^0 \simeq 1.288,\ \tau_y^a = 1.1, \tau_y^b \simeq 0.911$$

and

$$\tau_x^a \simeq 0.682,\ \tau_x^b \simeq 0.911, \tau_x^b \simeq 1.099.$$

[5] It is already confirmed that the same shape of the bifurcation diagrams are obtained regardless the particular values of the inital functions.

and the blue bifurcation diagram when the initial functions are identical,

$$\phi_x(t) = x^e + 0.1 \text{ and } \phi_y(t) = y^e + 0.1.$$

Since the blue diagram is placed on the red one in Figure 5, the two are identical for $\tau < \tau^b$ and $\tau > \tau^s (\simeq 1.106)$[6] while they are different for $\tau^b < \tau < \tau^s$. We observe only the red one for a while and refer to the blue one shortly after. According to Lemma 4, the one-delay system has the critical value of the delay, $\tau_{*,0}$ at which stability is lost. On the other hand, the diagonal of Figure 4(A) crosses the concave-shaped stability curve at $\tau_x^b = \tau_y^b = \tau^b (\simeq 0.907)$ at which the steady state loses stability. In a natural consequence, $\tau_{*,0} = \tau^b$. As shown in Figure 5(A), stability is lost at τ^b and periodic solutions are obtained for $\tau > \tau^b$. The numerical result agrees with the analytical result obtained in Lemma 4. We now turn attention to the difference of the two curves in interval (τ^b, τ^s). This difference implies that the steady state is stable along the blue curve while it bifurcates to a periodic behavior along the red curve. In other word, the steady state coexists with periodic solutions or multistability emerges. Furthermore, interesting phenomenon is observed in Figure 5(B) in which for $\tau > \tau^s$, a trajectory with the same initial functions seems to quickly converge to the steady state denoted by the red line but turns out eventually to converge to a periodic solution, transiently stable but finally unstable. These findings are obtained numerically.

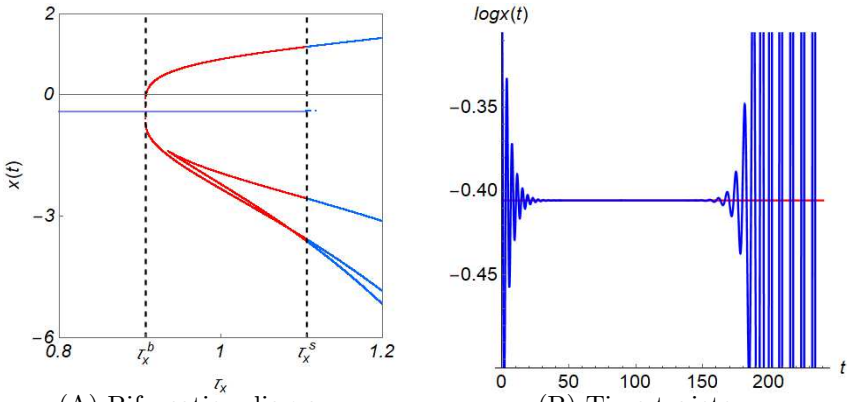

(A) Bifurcation diagram (B) Time trajetory

Figure 5. Dynamics in the one-delay system

In the second example, we examine the case of $\tau_x \neq \tau_y$. In particular, fixing $\tau_y = \tau_y^a$, the value of τ_x is increased along the horizontal dotted line at τ_y^a from 0 to 3/2 in Figure 4(A). The resultant bifurcation diagram is given in Figure 6(A) and the phase diagram with $\tau_x = 1.15$ in Figure 6(B). As usual, dynamics becomes more complicated via a quasi period-doubling cascade with

[6] The value of τ^s is numerically determined while the value of τ^b is analytically obtained.

some windows as the value of τ_x increases.

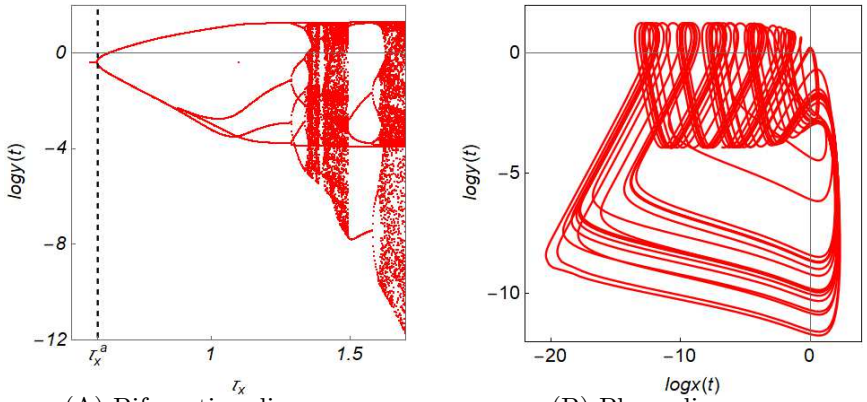

(A) Bifurcation diagram (B) Phase diagram

Figure 6. Dynamics of the second example

In the third example, we confirm the numerical results obtained by SS from a different view point. Figure 7 presents a bifurcation diagram with respect to τ_y that is increased from 0.5 to 0.9, given $\tau_x = 1.6$. As seen in Figure 5(A), the point $(\tau_x, \tau_y) = (1.6, 0)$ is located outside of the yellow region. Thus those points on the vertical line at $\tau_x = 1.6$ are unstable. The dotted vertical lines stand at $\tau_y^a = 0.6$, $\tau_y^b = 0.77$, $\tau_y^c = 0.85$ and $\tau_y^d = 0.85$, those of which are taken by SS in their Figure 2(a), Figure 2(b), Figure 3 and Figure 4(b). The bifurcation diagram indicates the birth of limit cycle for $\tau_y = \tau_y^a$, a two period cycle for $\tau_y = \tau_y^b$, and complicated dynamics for $\tau_y = \tau_y^c$ and $\tau_y = \tau_y^d$.

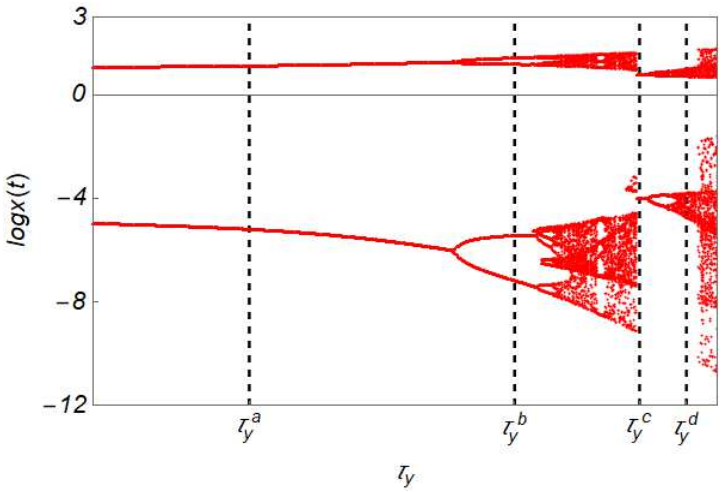

,

Figure 7. Bifurcation diagram with respect to τ_y, $\tau_x = 1.6$

5.2 Asymmetric Case

In this subsection, Specification II is used for which $\alpha_x > \alpha_y$, when the species are asymmetric. In the fourth example, we take the one-delay model again and the value of τ is increased along the diagonal in Figure 4(B) that crosses the stability switching curve at $\tau_x^b = \tau_y^b \simeq \tau^b \simeq 0.911$. It is seen in Figure 8(A) that the one-delay system can generate complicated dynamics as the value of τ becomes larger than about 1.5. In the fifth and final example, τ_y is fixed at $\tau_y = \tau_y^a = 1.1$ and τ_x is increased along the horizontal dotted line at τ_y^a. The resultant bifurcation diagram is given in Figure 8(B) that is distorted but not so much different than Figure 6 in the symmetric case.

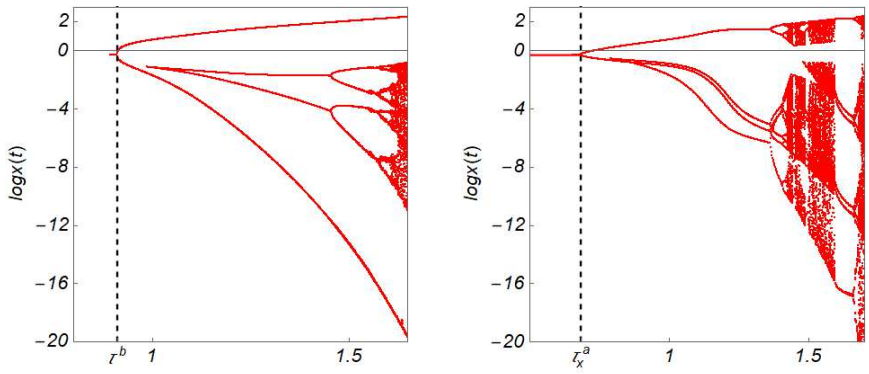

(A) $\tau_x = \tau_y$ (B) $\tau_x \neq \tau_y$

Figure 8. Bifurcation diagrams in the fourth and fifth examples

6 Concluding Remarks

The Lotka-Volterra competition system was examined and the effect of two time delays was analyzed. It was first demonstrated that the steady state is locally asymptotically stable without delays. If the delays are equal, then the model becomes a one-delay system. The threshold value of the delay was determined when stability was lost. If the delays are different, then a two-delay system is obtained. The stability switching curves were analytically determined and verified numerically. The numerical results showed that the unstable two-delay system may exhibit periodic behavior, multistability, quasi-period doubling cascade and even complicated dynamics depending on model parameters.

References

Hutchinson, G., Circular causal systems in ecology, *Annals of the New York Academy of Sciences*, 50, 221-246, 1948.

Lin, X. and Wang, E., Stability analysis of delay differential equations with two discrete delays, *Canadian Applied Mathematics Quarterly*, 20, 579-532, 2012.

Matsumoto, A. and Szidarovszky, F., Stability switching curves in a Lotka-Volterra competition system with two delays, IERCU #310, 2019. https://www.chuo-u.ac.jp//research/institute/publication/discussion.

Matsumoto, A. and Szidarovszky, F., *Dynamic oligopolies with time delays*, Springer-Verlag, Tokyo, 2018.

May, R., Time delay versus stability in population models with two and three trophic levels, *Ecology*, 54, 315-325, 1973.

Shibata, A. and Saito, N., Time delays and chaos in two competing species, *Mathematical Biosciences*, 51, 199-211, 1980.

Song, Y., Han, M. and Peng, Y., Stability and Hopf bifurcations in a competitive Lotka-Volterra system with two delays, *Chaos, Solitions and Fractals*, 22, 1139-1148, 2004.

Zhang, J., Stability and bifurcation periodic solutions in a Lotka-Volterra competition system with multiple delays, *Nonlinear Dynamics*, 70, 849-860, 2012.

Zhang, J., Jin, Z., Yan, J. and Sun, G., Stability and Hopf bifurcation in a delayed competition system, *Nonlinear Analysis*, 70, 658-670, 2009.